



Economic plant-wide control design with backoff estimations using internal model control

David A. Zumoffen^{*,1}, Lautaro Braccia, Alejandro G. Marchetti²

Process Systems Engineering Group (PSEG), French-Argentine International Center for Information and Systems Sciences (CIFASIS), CONICET-UNR,
27 de Febrero 210 bis, (S2000EZP) Rosario, Argentina³



ARTICLE INFO

Article history:

Received 16 July 2015

Received in revised form 27 January 2016

Accepted 10 February 2016

Available online 28 February 2016

Keywords:

Process control

Plant-wide control

Control structure selection

Backoff approach

ABSTRACT

Economic optimal operation typically involves operating as close as possible to the active constraints. However, in the presence of disturbances it is necessary to back-off from the constraints in order to avoid violating them. The backoff approach aims at selecting the control structure that minimizes the economic loss associated with the required constraint backoffs. This paper revisits the backoff approach and proposes a framework for estimating the constraint backoffs based on well-known elements of internal model control (IMC) theory, such as an automatic procedure for tuning the IMC low-pass filters, a stability condition, and an uncertainty representation based on diagonal input multiplicative uncertainty. Since the constraint backoffs are estimated using a linear dynamic model, the inclusion of input multiplicative uncertainty allows introducing conservatism in the estimation of the backoffs, which is required in order to avoid constraint violations. A forced-circulation evaporator benchmark problem is used to illustrate the approach.

© 2016 Elsevier Ltd. All rights reserved.

1. Introduction

In the process industries, an important design decision concerns the selection of an appropriate control structure (CS). Plantwide control (PWC) is a well-known research topic that addresses the decisions involved in control structure design [1–3]. Typical decisions involve the appropriate selection of the following elements: the controlled variables (CVs); the manipulated variables (MVs); the input–output pairing between these sets; and various characteristics associated with the controller itself, such as the interaction degree (diagonal, sparse, full); the control policy (decentralized or centralized); the controller technology (classical or advanced); and controller tuning. There are several approaches in the literature addressing the PWC problem in many different contexts and by using many different tools. Common procedures involve heuristic tools, model-based optimization, controllability assessments,

steady-state indexes, etc. A good review of these techniques can be found in Skogestad and Postlethwaite [1] and Rangaiah and Kariwala [2].

The attempts to integrate control structure selection, process design, and optimal process operation have demonstrated the need to parameterize the controller structure in some suitable manner. Some of the approaches that have been proposed for this purpose are the following ones: decentralized proportional-integral (PI) control [4], internal model control (IMC) [5], Q-parameterization [6], and model predictive control (MPC) [7,8]. The last three strategies have strong structural resemblances between them, in particular when the unconstrained case is considered. The classical IMC theory is a useful and well-known tool for controller design. Moreover, there are several developments in this area that serve to analyze tuning, performance, stability, and robustness [9]. The IMC design procedure allows to represent single-input single-output (SISO), as well as multiple-input multiple-output (MIMO) controllers easily by mean of the respective process model selected. In the MIMO case, the controller interaction (decentralized, full or sparse) can be investigated by defining a particular structural plant-model mismatch [10]. Due to all these interesting characteristics, the IMC approach becomes an excellent option for making control structure design decisions.

Among model-based optimization approaches, the use of dynamic optimization has been proposed in order to determine the most economic design that satisfies all the operability

* Corresponding author.

E-mail addresses: zumoffen@cifasis-conicet.gov.ar (D.A. Zumoffen), braccia@cifasis-conicet.gov.ar (L. Braccia), marchetti@cifasis-conicet.gov.ar (A.G. Marchetti).

¹ Also with Universidad Tecnológica Nacional – FRRo, Zeballos 1341, (S2000BQA) Rosario, Argentina.

² Present address: Laboratoire d'Automatique, Ecole Polytechnique Fédérale de Lausanne, Lausanne CH-1015, Switzerland.

³ Tel.: +54 341 4237248 304; fax: +54 341 482 1772.

constraints in the presence of bounded disturbances [11–13]. The optimum operating point is often located at the intersection of the active constraints. However, in the presence of disturbances it is necessary to include safety margins or backoffs in order to avoid constraint violations. The size of the backoffs depends on the variability of the constrained variables in the neighbourhood of the constraint boundaries for the closed-loop controlled system. The backoff approach for process control structure selection is based on the idea of selecting the control structure that minimizes the economic loss associated with the required constraint backoffs [4,14–16]. In these works, controller design is avoided by assuming perfect control. Heath et al. [4] also propose a more realistic approach wherein the constraint backoffs are estimated using decentralized PI controllers.

In this paper, we propose an alternative procedure for process control structure selection based on the backoff methodology, wherein the dynamic constraint backoffs are computed using IMC theory for parameterizing the controller. In this context, the tuning rules, the potential controller interaction, and the stability/robustness at closed-loop, can be evaluated in an unified framework. Although this article presents an analysis for decentralized and full controller interaction, the IMC structure allows to extend the methodology to sparse controllers [10]. The uncertainty representation based on diagonal input multiplicative uncertainty is proposed in order to introduce robustness in the estimation of the constraint backoffs. The overall problem can be formulated as a mixed-integer nonlinear program (MINLP). In this paper, a stochastic sequential global search approach based on genetic algorithms (GA) is proposed as solution strategy. In addition, a deterministic approach based on classical optimization tools is also tested in the Appendix. The performance of the proposed strategy is illustrated by means of a forced-circulation evaporator process.

The paper is arranged in the following order. Section 2 formulates the economic optimization problem, and introduces the different elements that are required for the approach proposed in this paper. Section 3 describes the methodology proposed in this paper, which consists in implementing the constraint back-off approach using IMC theory for parameterizing the controller. The overall control structure selection algorithm is presented. In Section 4 the evaporator process is presented and the suggested procedure is applied. Several optimization results and dynamic simulations are presented in order to illustrate the overall methodology. Finally, Section 5 concludes the paper.

2. Preliminaries

2.1. Economic optimization problem

The open-loop behavior of the plant is represented by the following system of differential-algebraic equations:

$$\mathbf{f}_D(\dot{\mathbf{x}}, \mathbf{x}, \mathbf{w}, \mathbf{u}, \mathbf{d}) = \mathbf{0}, \quad (1a)$$

$$\mathbf{f}_A(\mathbf{x}, \mathbf{w}, \mathbf{u}, \mathbf{d}) = \mathbf{0}, \quad (1b)$$

$$\mathbf{y} = \mathcal{F}(\mathbf{x}, \mathbf{w}, \mathbf{u}, \mathbf{d}), \quad (1c)$$

where $\mathbf{x} \in IR^{n_x}$ is the vector of state variables, $\mathbf{w} \in IR^{n_w}$ is the vector of algebraic variables, $\mathbf{u} \in IR^{n_u}$ is the vector of input variables, $\mathbf{d} \in IR^{n_d}$ is the vector of uncertain parameters and disturbances, and $\mathbf{y} \in IR^{n_y}$ is the vector of measured output variables.

Continuously operating plants are typically designed to operate at steady-state conditions. The optimum steady-state operating point is given by the solution of the following nonlinear program (NLP):

$$\mathbf{u}^*(\mu, \mathbf{d}) = \underset{\mathbf{u}}{\operatorname{argmin}} \quad J(\mathbf{x}, \mathbf{w}, \mathbf{u}, \mathbf{d}) \quad (2a)$$

$$\text{s.t. } \mathbf{f}_D(\mathbf{0}, \mathbf{x}, \mathbf{w}, \mathbf{u}, \mathbf{d}) = \mathbf{0}, \quad (2b)$$

$$\mathbf{f}_A(\mathbf{x}, \mathbf{w}, \mathbf{u}, \mathbf{d}) = \mathbf{0}, \quad (2c)$$

$$\mathbf{y}^L + \boldsymbol{\mu}_y \leq \mathbf{y} = \mathcal{F}(\mathbf{x}, \mathbf{w}, \mathbf{u}, \mathbf{d}) \leq \mathbf{y}^U - \boldsymbol{\mu}_y, \quad (2d)$$

$$\mathbf{u}^L + \boldsymbol{\mu}_u \leq \mathbf{u} \leq \mathbf{u}^U - \boldsymbol{\mu}_u, \quad (2e)$$

where J is the economic objective function (or cost) to be minimized, \mathbf{y}^L and \mathbf{y}^U are the lower and upper bounds on the output variables, and \mathbf{u}^L and \mathbf{u}^U are the lower and upper bounds on the input variables. The vectors $\boldsymbol{\mu}_y \in IR^{n_y}$ and $\boldsymbol{\mu}_u \in IR^{n_u}$, with $\boldsymbol{\mu}_y, \boldsymbol{\mu}_u \geq \mathbf{0}$, denote the output and input constraint backoffs, respectively. These constraint backoffs are typically included in order to avoid dynamic constraints violations due to perturbations. Alternatively, the output and input constraints (2d) and (2e) can be written collectively as the constraints

$$\mathbf{g}(\mathbf{x}, \mathbf{w}, \mathbf{u}, \mathbf{d}) + \boldsymbol{\mu} \leq \mathbf{0}, \quad (3)$$

with the constraint backoffs $\boldsymbol{\mu} \geq \mathbf{0}$. Note that \mathbf{g} may also include constraints for unmeasured predicted variables.

We denote by $\mathbf{u}^*(\mu, \mathbf{d})$ the optimal input as a function of the constraint backoffs and the disturbances. The constraint backoff vector $\boldsymbol{\mu}$ is said to be *implementable* if for that $\boldsymbol{\mu}$ there exists a feasible solution to Problem (2) for any $\mathbf{d} \in \mathcal{D}$, where the disturbance set \mathcal{D} is considered to be a box set of the form $\mathcal{D} = \{\mathbf{d} \in IR^{n_d} : \mathbf{d}_{\min} \leq \mathbf{d} \leq \mathbf{d}_{\max}\}$.

2.2. Plantwide control problem

Let us consider a stable (or stabilized) linear process model with n_u inputs, n_y outputs, and n_d disturbance variables, represented as

$$\mathbf{y}(s) = \mathbf{G}(s)\mathbf{u}(s) + \mathbf{D}(s)\mathbf{d}(s), \quad (4)$$

where $\mathbf{y}(s)$, $\mathbf{u}(s)$, and $\mathbf{d}(s)$ are the vectors of output, input, and disturbance variables, respectively, and $\mathbf{G}(s)$ and $\mathbf{D}(s)$ are transfer functions matrices (TFM) of dimensions $(n_y \times n_u)$ and $(n_y \times n_d)$. We assume that the linear model (4) is obtained at the nominal optimum operating point $\mathbf{u}^*(\mathbf{0}, \mathbf{d}_n)$, i.e., the solution to Problem (2) with zero offset ($\boldsymbol{\mu} = \mathbf{0}$) and nominal disturbances \mathbf{d}_n . Let us consider the following partitioning of the variables

$$\mathbf{y}(s) = \begin{bmatrix} \mathbf{y}_s(s) \\ \mathbf{y}_r(s) \end{bmatrix} = \begin{bmatrix} \mathbf{G}_s(s) & \mathbf{G}_s^*(s) \\ \mathbf{G}_r(s) & \mathbf{G}_r^*(s) \end{bmatrix} \begin{bmatrix} \mathbf{u}_s(s) \\ \mathbf{u}_r(s) \end{bmatrix} + \begin{bmatrix} \mathbf{D}_s(s) \\ \mathbf{D}_r(s) \end{bmatrix} \mathbf{d}(s) \quad (5)$$

where $\mathbf{G}_s(s)$ is the square $(n_q \times n_q)$ subprocess to be controlled, $\mathbf{u}_s(s) \in IR^{n_q}$ is the selected subset of MVs used for controlling the selected CVs $\mathbf{y}_s(s) \in IR^{n_q}$, $\mathbf{u}_r(s) \in IR^{n_u-n_q}$ are the remaining input variables, which are not used for control purposes, $\mathbf{y}_r(s) \in IR^{n_y-n_q}$ are uncontrolled output variables (UVs), and $\mathbf{G}_s^*(s)$, $\mathbf{G}_r^*(s)$, $\mathbf{D}_s(s)$, $\mathbf{D}_r(s)$ are transfer function matrices of appropriate dimensions.

Note that the partitioning in Eq. (5) depends on $n_q \leq \min(n_u, n_y)$, which represents the number of controlled variables. Let us consider the parametrization vector $\mathcal{Z} = [\mathbf{c}_O, \mathbf{c}_I, n_q]$, where $\mathbf{c}_O = [c_1^O, \dots, c_{n_y}^O]$ and $\mathbf{c}_I = [c_1^I, \dots, c_{n_u}^I]$ are two vectors for which each component c_j^O (or c_j^I) is a binary decision variable, and $0 < n_q \leq \min(n_y, n_u)$ represents an integer variable. The subprocess $\mathbf{G}_s(s)$ to be controlled can then be selected as

$$\mathbf{G}_s^z(s) = \mathbf{T}_O \mathbf{G}(s) \mathbf{T}_I \quad (6)$$

with

$$\|\mathbf{c}_O\|_1 = \|\mathbf{c}_I\|_1 = n_q, \quad \mathbf{T}_O = \text{nre}[\text{diag}(\mathbf{c}_O)], \quad \mathbf{T}_I = \text{nce}[\text{diag}(\mathbf{c}_I)]. \quad (7)$$

The first equation in (7) is the condition to guarantee a square control problem. Note that $\|\cdot\|_1$ is the 1-norm for vectors, i.e., the sum of the absolute values of the elements of the vector. The matrices \mathbf{T}_O and \mathbf{T}_I are selection matrices. The operator $\text{diag}(\mathbf{c})$ returns

a diagonal matrix with the entry vector \mathbf{c} in its main diagonal. The operators $nre(\cdot)$ and $nce(\cdot)$ take a square matrix as input argument and return a generally non square matrix, wherein the null rows are eliminated, and the null columns are eliminated, respectively. Similarly, the remaining matrices $\mathbf{G}_r^Z(s)$, $\mathbf{D}_s^Z(s)$, and $\mathbf{D}_r^Z(s)$ can also be computed from the parameterization vector Z by defining appropriate selection matrices.

The selection of the subprocess to be controlled is just the first step in the PWC design problem. For each specific choice of $\mathbf{G}_s(s)$ the input–output pairing should also be computed. For a given parameterization vector Z , the input–output pairing may be computed based on the well-known relative gain array (RGA) number approach [1]. The main idea here is to find the column permutations in $\mathbf{G}_s^Z(s)$ that minimize the RGA number. This procedure guarantees diagonal dominance, which is a desirable characteristic for decentralized control structure designs. Given the steady-state gain matrix $\mathbf{G} \in \mathbb{R}^{nq \times nq}$, the RGA matrix is defined as:

$$\Lambda(\mathbf{G}) = \mathbf{G} \otimes (\mathbf{G}^{-1})^T,$$

where \otimes denotes the element-by-element multiplication (the Hadamard or Schur product). In turn, the RGA number is defined as:

$$\Lambda_n(\mathbf{G}) = \|\Lambda(\mathbf{G}) - \mathbf{I}\|_{\text{sum}}.$$

The sum-norm is defined as $\|A\|_{\text{sum}} = \sum_{ij} |a_{ij}|$, where a_{ij} is the ij -element of A . The problem to be solved consists in finding the column permutations on matrix \mathbf{G} that minimize the RGA number. This problem can be formulated as follows:

$$\begin{aligned} \min \quad & \Lambda_n(\mathbf{GP}) = \|\Lambda(\mathbf{G})\mathbf{P} - \mathbf{I}\|_{\text{sum}} \\ \text{s.t.} \quad & \mathbf{P} = [p_{ij}]; \quad p_{ij} \in \{0, 1\}, \quad \forall i, j \\ & \sum_i p_{ij} = 1, \quad \forall j; \quad \sum_j p_{ij} = 1, \quad \forall i \end{aligned} \quad (8)$$

The decision variables are the binary variables $p_{ij} \in \{0, 1\}, \forall i, j \in \{1, \dots, n_q\}$. \mathbf{P} is a permutation matrix. Note that, $\Lambda(\mathbf{GP}) = \Lambda(\mathbf{G})\mathbf{P}$, from the permutation property of RGA [1].

The remaining design decisions of the PWC problem are related to the characteristics of the controller itself (interaction degree, decentralized/centralized, tuning, classical/advanced). All these decisions drastically increase the size of the potential solution space in the PWC problem.

2.3. Multivariable control structure based on IMC

In this section, we describe the use of internal model control (IMC) in the context of control structure selection. For a given control structure Z , and considering that the input variables $\mathbf{u}_r(s)$ are not used for control purposes, the process model in Eq. (5) becomes:

$$\begin{bmatrix} \mathbf{y}_s^Z(s) \\ \mathbf{y}_r^Z(s) \end{bmatrix} = \begin{bmatrix} \mathbf{G}_s^Z(s) \\ \mathbf{G}_r^Z(s) \end{bmatrix} \mathbf{u}_s^Z(s) + \begin{bmatrix} \mathbf{D}_s^Z(s) \\ \mathbf{D}_r^Z(s) \end{bmatrix} \mathbf{d}(s). \quad (9)$$

The generalized IMC structure is shown in Fig. 1. The IMC controller is defined as $\mathbf{G}_c^Z(s) = (\tilde{\mathbf{G}}_s^Z(s))^{-1} \mathbf{F}(s)$, where $\tilde{\mathbf{G}}_s^Z(s)$ is the invertible part of the process model $\mathbf{G}_s^Z(s)$, and $\mathbf{F}(s)$ is a diagonal low-pass filter matrix. The main goal of $\mathbf{F}(s)$ is ensure that $\mathbf{G}_c^Z(s)$ is a feasible (proper) function [10,17]. The controlled, uncontrolled, and manipulated variables are modelled as:

$$\begin{aligned} \mathbf{y}_s^Z(s) &= \tilde{\mathbf{G}}_s^Z(s) \mathbf{G}_c^Z(s) \mathbf{y}_s^{\text{sp}}(s) + \left[\mathbf{I} - \tilde{\mathbf{G}}_s^Z(s) \mathbf{G}_c^Z(s) \right] \\ &\times \left[\mathbf{A}_s^Z(s) \mathbf{y}_s^{\text{sp}}(s) + \mathbf{B}_s^Z(s) \mathbf{d}(s) \right], \end{aligned} \quad (10)$$

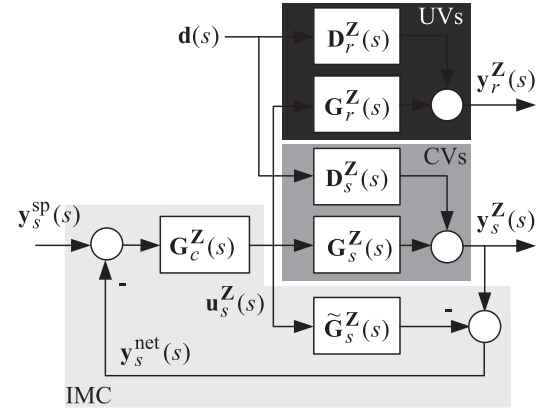


Fig. 1. Generalized IMC structure.

$$\begin{aligned} \mathbf{y}_r^Z(s) &= \mathbf{G}_r^Z(s) \mathbf{G}_c^Z(s) [\mathbf{I} - \mathbf{A}_s^Z(s)] \mathbf{y}_s^{\text{sp}}(s) \\ &+ [\mathbf{D}_r^Z(s) - \mathbf{G}_r^Z(s) \mathbf{G}_c^Z(s) \mathbf{B}_s^Z(s)] \mathbf{d}(s), \end{aligned} \quad (11)$$

$$\mathbf{u}_s^Z(s) = \mathbf{G}_c^Z(s) \mathbf{y}_s^{\text{sp}}(s) - \mathbf{G}_c^Z(s) [\mathbf{A}_s^Z(s) \mathbf{y}_s^{\text{sp}}(s) + \mathbf{B}_s^Z(s) \mathbf{d}(s)]. \quad (12)$$

with

$$\mathbf{A}_s^Z(s) = \left[\mathbf{I} + \left(\mathbf{G}_s^Z(s) - \tilde{\mathbf{G}}_s^Z(s) \right) \mathbf{G}_c^Z(s) \right]^{-1} \left(\mathbf{G}_s^Z(s) - \tilde{\mathbf{G}}_s^Z(s) \right) \mathbf{G}_c^Z(s), \quad (13)$$

$$\mathbf{B}_s^Z(s) = \left[\mathbf{I} + \left(\mathbf{G}_s^Z(s) - \tilde{\mathbf{G}}_s^Z(s) \right) \mathbf{G}_c^Z(s) \right]^{-1} \mathbf{D}_s^Z(s). \quad (14)$$

Since the controller $\mathbf{G}_c^Z(s)$ depends on the selected process model $\tilde{\mathbf{G}}_s^Z(s)$, the following model parametrization can be used for selecting a given controller interaction

$$\tilde{\mathbf{G}}_s^{Z\Gamma}(s) = \tilde{\mathbf{G}}_s^Z(s) \otimes \Gamma, \quad \text{with } \Gamma = [\gamma_{ij}]_{n_q \times n_q} \quad (15)$$

where \otimes represents the Hadamard product and γ_{ij} is a binary variable indicating if the ij th entry is selected ($\gamma_{ij} = 1$) or not ($\gamma_{ij} = 0$). Using this parameterization, the IMC controller results $\mathbf{G}_c^{Z\Gamma}(s) = (\tilde{\mathbf{G}}_s^{Z\Gamma}(s))^{-1} \mathbf{F}(s)$.

Henceforth, only two alternative structures will be used for Γ , which correspond to the well-known controllers with decentralized (Γ is a diagonal unitary matrix) and full (Γ is a full unitary matrix) interaction, respectively. The parameterization vector Z previously introduced can be augmented as $Z = [\mathbf{c}_O, \mathbf{c}_I, n_q, v]$, where the new binary variable v indicates a MIMO controller design based on decentralized ($v = 0$) or full ($v = 1$) interaction.

A restriction on the structure Z can be included in order to enforce a stability condition on the closed-loop system. In this regard, Garcia and Morari [17] developed the following steady-state criterion

$$\operatorname{Re} \left[\lambda_i \left(\mathbf{G}_s(\tilde{\mathbf{G}}_s^{Z\Gamma})^{-1} \right) \right] > 0, \quad \text{with } i = 1, \dots, n_q, \quad (16)$$

where $\operatorname{Re}[\cdot]$ is the real part function and $\lambda_i(\cdot)$ is the i th eigenvalue, in order to test if a multivariable control structure based on IMC is stabilizable. In other words, if Eq. (16) is satisfied, then there exists some filter matrix \mathbf{F} which stabilizes the closed-loop system.

2.3.1. Controller tuning

In the context of IMC, the time constant of the low-pass filters included in the filter matrix $\mathbf{F}(s)$ define the final setting of the controller. First, let us consider the adjustment of the filter transfer

function matrix $\mathbf{F}(s)$ using a decentralized multivariable IMC structure. The tuning procedure proposed by Garcia and Morari [17,18] is adopted in this work. This tuning procedure requires the approximated model $\tilde{G}(s) = [\tilde{g}_{ij}(s)]$ to be selected as first-order transfer functions, with or without dead-time information. Thus, the model component associated with the input–output pairing $u_j - y_i$ is given by $\tilde{g}_{ij}(s) = k_m^{ij}/(\tau_m^{ij}s + 1)$ (without dead time), and the corresponding filter component is selected as

$$f_{ij} = 1/(\tau_f^{ij}s + 1), \quad \text{where } \tau_f^{ij} = \tau_m^{ij}/\nu^{ij}, \quad \text{and } \nu^{ij} > 0.$$

It is worth mentioning that ν^{ij} is directly related with the desired closed-loop response of the corresponding pairing. In general, values of ν^{ij} greater than one improve the servo/regulator response compared with the open-loop case. On the other hand, note that ν^{ij} cannot be increased indefinitely since some saturation problems, due to aggressive responses in the corresponding MV, could appear. Furthermore, if the associated model component $g_{ij}(s)$ presents dead time (delay) θ_{ij} , the filter time constant must be selected as $\tau_f^{ij} > \theta_{ij}$ in order to satisfy the robustness/stability condition. It is clear that this situation imposes the bounds $0 < \nu^{ij} < \tau_m^{ij}/\theta_{ij}$.

In the case of a centralized control structure (full interaction) the controller tuning is more involved, and it usually has more drastic influences on the final closed-loop performance. The full interaction case can be tuned conservatively by considering the following generalization: $\tau_f^{ij} > \max(\theta_{ij})$, $\forall i = 1, \dots, n_q$, that is, by considering the maximum delay along the j th input channel [19].

2.4. The backoff methodology

In order for the regulatory control system to be able to avoid violating the constraints in the presence of fast acting disturbances, it is necessary to move the optimum operating point inside the feasible region by backing-off from the active (and nearly active) constraints. The backoff methodology for selecting process control structures is based on the idea of using the economic loss associated with the required constraint backoffs as a measure for ranking different control structures [4,14,15].

The economic loss is defined at the nominal values of the disturbances as:

$$\text{Loss}^\mu := J^*(\mu, \mathbf{d}_n) - J^*(\mathbf{0}, \mathbf{d}_n), \quad (17)$$

where $J^*(\mu, \mathbf{d}_n)$ is the optimal cost of Problem (2a) with constraint backoffs μ and nominal disturbances \mathbf{d}_n , while $J^*(\mathbf{0}, \mathbf{d}_n)$ is the nominal optimal cost with zero backoffs.

For a given regulatory control system, the maximum deviation of the j th constrained variable from its nominal value under the effect of disturbances over the time horizon of interest, can be defined as [4]:

$$\mu_j = \max_{t \in T} \max_{\mathbf{d}(t) \in \mathcal{D}} g_j(\mathbf{x}(t), \mathbf{w}(t), \mathbf{u}(t), \mathbf{d}(t), \mathcal{Z}) - g_j(\mathbf{x}_n, \mathbf{w}_n, \mathbf{u}_n, \mathbf{d}_n), \\ \text{for } j = 1, \dots, n_g, \quad (18)$$

where $\mathbf{u}_n = \mathbf{u}^*(\mathbf{0}, \mathbf{d}_n)$ denotes the optimum nominal input. Problem (18) constitutes a dynamic optimization problem for the controlled plant under general uncertainty. Notice that the size of the backoff computed in (18) depends on the choice of the regulatory control system, including the control structure, the type of controller, and the specific technique used for selecting the controller's parameters. Once these choices are made, the control structure

selection problem can be formulated as follows:

$$\begin{aligned} \min_{\mathbf{u}, \mathcal{Z}} \quad & \text{Loss} = J(\mathbf{x}, \mathbf{w}, \mathbf{u}, \mathbf{d}_n) - J^*(\mathbf{0}, \mathbf{d}_n) \\ \text{s.t.} \quad & \mathbf{f}_D(\mathbf{0}, \mathbf{x}, \mathbf{w}, \mathbf{u}, \mathbf{d}_n) = \mathbf{0}, \\ & \mathbf{f}_A(\mathbf{x}, \mathbf{w}, \mathbf{u}, \mathbf{d}_n) = \mathbf{0}, \\ & \mathbf{g}(\mathbf{x}, \mathbf{w}, \mathbf{u}, \mathbf{d}_n) + \boldsymbol{\mu} \leq \mathbf{0}, \\ & \mu_j = \max_{t \in T} \max_{\mathbf{d}(t) \in \mathcal{D}} g_j(\mathbf{x}(t), \mathbf{w}(t), \mathbf{u}(t), \mathbf{d}(t), \mathcal{Z}) - g_j(\mathbf{x}_n, \mathbf{w}_n, \mathbf{u}_n, \mathbf{d}_n), \\ & \text{forall } j = 1, \dots, n_g. \end{aligned} \quad (19)$$

The variables \mathbf{x} , \mathbf{w} , and \mathbf{u} define a steady-state operating point, while $\mathbf{x}(t)$, $\mathbf{w}(t)$, and $\mathbf{u}(t)$ are the time-varying variables used to compute the backoffs in Problem (18). Notice that Problem (19) is the combination of Problems (2) and (18). In other words, the loss associated with a given control structure is obtained by first solving Problem (18) and then using the computed backoff in Problem (2) for the nominal disturbance values.

In this work, it is assumed that the regulatory controllers are designed with integral action. Otherwise, the equations modeling the steady-state behavior of the controlled plant should be included in Problem (19), instead of the open-loop steady-state model. With this assumption, the choice of the control structure defined by \mathcal{Z} affects the loss only through the constraint backoff associated with that control structure, which is obtained by solving Problem (36). Notice that, in evaluating the constraint backoffs using Problem (18), the setpoints for the selected CVs and the values of the fixed variables correspond to the nominal optimum values obtained with zero offset. However, in implementing the controller, the setpoints for the CVs should be selected as the values obtained at the optimum operating point given by the solution of Problem (19), i.e., the backed-off setpoints.

In order to solve Problem (18), a number of simplifying assumptions and approximations have been proposed in the literature [15]. One important approximation is to linearize the controlled system dynamics at the nominal optimum steady state:

$$\mathbf{g}(s) = \Phi^{\mathcal{Z}}(s)\mathbf{d}(s) \quad (20)$$

where $\mathbf{g}(s)$ and $\mathbf{d}(s)$ are the Laplace transforms of the constraint and disturbance deviations, respectively, and $\Phi^{\mathcal{Z}}(s)$ is the corresponding transfer function matrix of the closed-loop system. Perkins and co-authors [4,14,15,20] proposed to estimate the constraint back-offs by considering the following frequency response bounds:

$$\max_t |\delta g_i(t)| \leq \max_\omega |\phi_{ij}(\omega)| |\Delta d_j| = \|\phi_{ij}(s)\|_\infty |\Delta d_j| \quad (21)$$

where the maximum deviation of the constrained variable $g_i(t)$ due to a step change $\Delta d_j/s$ in the j th disturbance is bounded by the maximum of the magnitude in the frequency domain. If all the disturbances are considered, the maximum deviation results from applying the superposition principle:

$$\max_t |\delta g_i(t)| \leq [\|\phi_{i1}(s)\|_\infty \|\phi_{i2}(s)\|_\infty \dots \|\phi_{in_u}(s)\|_\infty] [|\Delta d_1| |\Delta d_2| \dots |\Delta d_n|]^T. \quad (22)$$

This way, the difficulty in solving Problem (18) can be greatly alleviated by using the upper bounds given by (22) as estimates of the constraint backoffs.

Problem (19) is a general formulation that defines the control structure selection problem in terms of the constraint backoffs. The main difficulty lies in how to pass from Problem (19) to a concrete strategy and problem formulation for control structure selection. This involves several decisions such as the simplifying assumptions and approximations made, the choice of the type of controller, the choice of an automatic controller tuning technique, the solution

strategy, etc. We next describe the approach proposed by Heath et al. [4], and subsequently, we present an alternative approach in Section 3.

Approach proposed by Heath et al. [4]

In Heath et al. [4] an important effort is made to reformulate Problem (19) as a mixed-integer linear program (MILP). This requires several linearizing approximations:

- (a) The frequency bounds given in (22) are estimated by decomposing the Laplace transform equations into their real and imaginary parts, and outer approximating the magnitude in the complex plane (which is nonlinear) using square box constraints, which are linear. A (finite) discretization in the frequency domain is performed, and the box constraints are evaluated at each discrete frequency value.
- (b) The NLP problem (2) is approximated as a linear program (LP). This involves a linearization of the cost function (2a), the model equations (2b), (2c), and the constraints (2d) (or (3)).

Formulating the problem as a MILP is very convenient from a computational point of view. However, solving the approximated problem does not guarantee obtaining the optimal solution of the original nonlinear problem. For instance, the LP approximation of Problem (2) limits the applicability of the MILP formulation to optimization problems for which the solution is completely determined by the intersection of the active constraints. A solution for which the number of active constraints is less than the number of inputs will not be captured.

Another important simplification used in Heath et al. [4] is the *perfect control assumption*. This assumption avoids the need to design the controller and to consider its effect on the plant dynamics. Basically, this assumption implies that, whenever an output variable is selected as a controlled variable, its corresponding constraint backoff is equal to zero. This has the disadvantage that, if all the active constraints correspond to output variables, the backoff approach loses its ‘raison d’être’ as an approach for control structure selection. Heath et al. [4] also propose a more realistic approach wherein the constraint backoffs are estimated using decentralized PI controllers.

3. Backoff approach based on IMC

In this section, we propose an alternative framework for control structure selection in the context of the backoff approach. Similar to the approach proposed by Heath et al. [4], we also depart from Problem (19) and we also simplify Problem (18) by considering a linearization of the controlled system and the estimation of the constraint backoffs based on (22). The difference lies in how we pass from Problem (19) to a concrete strategy for control structure selection. The proposed approach consists in estimating the constraint backoffs using automatically tuned IMC controllers. Also, we do not linearize the NLP Problem (2). This has the advantage of reducing the level of approximation, but it has the disadvantage of requiring to solve a more complex problem. The IMC framework allows to incorporate several elements of IMC theory in the context of the control structure selection problem.

3.1. Backoff estimation

In this section, we describe the estimation of the constraint backoffs using the IMC framework and tuning technique described in Section 2.3. For a given control structure \mathcal{Z} , the filter matrix $\mathbf{F}(s)$

can be tuned as indicated in Section 2.3. Considering the disturbance effects only, Eqs. (10)–(12) reduce to

$$\mathbf{y}_s^Z(s) = \Psi^Z(s)\mathbf{d}(s), \quad \Psi^Z(s) = \left[\mathbf{I} - \tilde{\mathbf{G}}_s^Z(s)\mathbf{G}_c^Z(s) \right] \mathbf{B}_s^Z(s), \quad (23)$$

$$\mathbf{y}_r^Z(s) = \Xi^Z(s)\mathbf{d}(s), \quad \Xi^Z(s) = \mathbf{D}_r^Z(s) - \mathbf{G}_r^Z(s)\mathbf{G}_c^Z(s)\mathbf{B}_s^Z(s), \quad (24)$$

$$\mathbf{u}_s^Z(s) = \Upsilon^Z(s)\mathbf{d}(s), \quad \Upsilon^Z(s) = -\mathbf{G}_c^Z(s)\mathbf{B}_s^Z(s), \quad (25)$$

where $\mathbf{B}_s^Z(s)$ is the matrix defined in (14). An estimate of the maximum deviations of the CVs \mathbf{y}_s^Z in response to disturbances can be obtained by applying the frequency response bound (22) to Eq.(23):

$$\begin{bmatrix} \max_t |y_{s,1}(t)| \\ \max_t |y_{s,2}(t)| \\ \vdots \\ \max_t |y_{s,n_q}(t)| \end{bmatrix} \leq \Psi_\infty^Z \begin{bmatrix} |\Delta d_1| \\ |\Delta d_2| \\ \vdots \\ |\Delta d_{n_d}| \end{bmatrix}, \quad \text{with} \\ \Psi_\infty^Z = \left[\|\psi_{ij}(s)\|_\infty \right]_{n_q \times n_d}. \quad (26)$$

Using the same approach, the maximum deviations of the UVs and the MVs can be estimated by defining the normed matrices Ξ_∞^Z and Υ_∞^Z , respectively. Thereby, the backoff estimation results

$$\boldsymbol{\mu}^Z = \begin{bmatrix} \boldsymbol{\mu}_{CV}^Z \\ \boldsymbol{\mu}_{UV}^Z \\ \boldsymbol{\mu}_{MV}^Z \end{bmatrix} = \begin{bmatrix} \Psi_\infty^Z \\ \Xi_\infty^Z \\ \Upsilon_\infty^Z \end{bmatrix} \begin{bmatrix} |\Delta d_1| \\ |\Delta d_2| \\ \vdots \\ |\Delta d_{n_d}| \end{bmatrix}, \quad (27)$$

where $\boldsymbol{\mu}_{CV}^Z$ and $\boldsymbol{\mu}_{UV}^Z$ are the backoff vectors for the controlled and uncontrolled output variables, respectively, and $\boldsymbol{\mu}_{MV}^Z$ represents the backoff vector for the manipulated inputs. The input variables that are not used as manipulated variables are fixed at their nominal optimum values and thus have zero backoff.

3.2. Robustness

The evaluation of the constraint backoffs $\boldsymbol{\mu}$ given in (27) is based on an approximate linear model of the real process. In order to avoid violating the constraints (when disturbances take place) due to the inevitable process model uncertainties, some conservatism should be introduced in the estimation of $\boldsymbol{\mu}$. In this paper, robust backoffs are computed by considering input multiplicative uncertainty [1]. In particular, the representation based on diagonal input uncertainties is very used because it considers the uncertainty or neglected dynamics in the individual input channels (actuators) or in the individual output channels (sensors). According to Skogestad and Postlethwaite [1] this type of diagonal uncertainty should always be considered because (i) it is always present and a PWC design which is sensitive to this uncertainty will not work in practice, and (ii) it often restricts achievable performance in multivariable control. Let us consider a particular component $g_{ij}(s)$ of the transfer function matrix $\mathbf{G}(s)$ corresponding to the nominal model. The component $g_{ij}(s)$ links the output $y_i(s)$ and the input $u_j(s)$. The corresponding uncertain component $g_{ij}^u(s)$, which is affected by the input multiplicative uncertainty, can be obtained as [1]:

$$g_{ij}^u(s) = g_{ij}(s)(1 + w_{ij}(s)\delta_j(s)), \quad \text{with } \| \delta_j(s) \|_\infty \leq 1 \quad (28)$$

where the multiplicative component $(1 + w_{ij}(s)\delta_j(s))$ is used to model the uncertainty introduced by physical systems such as amplifiers, signal converters, actuators, valves, etc.

When all the uncertain input channels are combined the complete uncertain process $\mathbf{G}^u(s)$ can be represented by considering the

nominal model $\mathbf{G}(s)$ as,

$$\begin{aligned}\mathbf{G}^u(s) &= \mathbf{G}(s)(\mathbf{I} + \mathbf{W}_I(s)\Delta_I(s)), \quad \text{with } \Delta_I(s) = \text{diag}\{\delta_j(s)\}, \\ \mathbf{W}_I(s) &= \text{diag}\{w_{lj}(s)\}\end{aligned}\quad (29)$$

Usually, the uncertainty in the j th input channel is represented by using a simple weighting function:

$$w_{lj}(s) = \frac{\tau^j s + r_0^j}{(\tau^j/r_\infty^j)s + 1} \quad (30)$$

where r_0^j is the relative uncertainty at steady state (at least 10%, i.e. $r_0^j = 0.1$), $1/\tau^j$ is approximately the frequency where the relative uncertainty reaches 100%, and r_∞^j is the relative uncertainty at higher frequencies (typically $r_\infty^j \geq 2$) [1].

Thus, the back-off evaluation presented in previous sections can be recomputed for the selected control structures by incorporating the input multiplicative uncertainty description suggested here. In fact, μ can be evaluated by considering the worst-case gain condition of $\mathbf{G}^u(s)$ given for $\|\Delta_I(s)\|_\infty = 1$. The closed-loop bandwidth is given by the controller tuning $1/\tau_f^{ij}$ and represents the natural zone where feedback control is effective. In this work, it is assumed that the controller tuning avoids working in the frequency range where the relative uncertainty reaches 100%, i.e. $1/\tau_f^{ij} < 1/\tau^j$.

3.3. Control structure selection problem

In this section we discuss how to group all the methodologies previously analyzed in a single optimization algorithm. The main objective is to minimize the loss index Loss^{μ^z} given in Eq. (17). This index quantifies the loss that results from operating the process at the backed-off operating point $\mathbf{u}^*(\mu, \mathbf{d}_n)$, with respect to the optimum nominal point $\mathbf{u}_n = \mathbf{u}^*(\mathbf{0}, \mathbf{d}_n)$ evaluated with zero backoff. The decision variables in the control structure selection problem correspond to the integer variables in the vector $\mathcal{Z} = [\mathbf{c}_O, \mathbf{c}_I, n_q, v]$ of dimension $(n_y + n_u + 2)$. The binary vectors \mathbf{c}_O and \mathbf{c}_I of dimensions n_y and n_u , respectively, parameterize the selection of CVs and MVs; the integer variable n_q defines the dimension/size of the multivariable controller; and the binary variable v indicates if the controller structure is decentralized (Γ_d) or full (Γ_f). The steps involved in the evaluation of Loss^{μ^z} for a given parameterization vector \mathcal{Z} are shown in Fig. 2, and briefly summarized next:

- (a) *Process partitioning*: The transfer function matrices $\mathbf{G}_s^z(s)$, $\mathbf{G}_r^z(s)$, $\mathbf{D}_s^z(s)$, and $\mathbf{D}_r^z(s)$ are constructed based on the values of \mathbf{c}_O , \mathbf{c}_I , and n_q .
- (b) *Pairing*: The input–output pairing is determined based on the RGA number.
- (c) *Design and tuning of IMC controller*: The controller is designed and tuned based on the above process partitioning and the filter matrix $\mathbf{F}(s)$. The tuning procedure is described in Section 2.3.1.
- (d) *Backoff evaluation*: The constraint backoffs μ^z are estimated from (27).
- (e) *Optimization problem*: The steady-state optimization problem (2) is solved for $\mu = \mu^z$ and $\mathbf{d} = \mathbf{d}_n$ in order to compute the nominal backed-off operating point $\mathbf{u}^*(\mu^z, \mathbf{d}_n)$ and the associated economic loss, Loss^{μ^z} .

The feasible solution map, $U(\cdot)$, and the domain of $U(\cdot)$, can be defined as [21]:

$$U(\mu) := \{\mathbf{u} \in IR^{n_u} : \text{ Eqs. (2b)–(2e) are satisfied with } \mathbf{d} = \mathbf{d}_n\}, \quad (31)$$

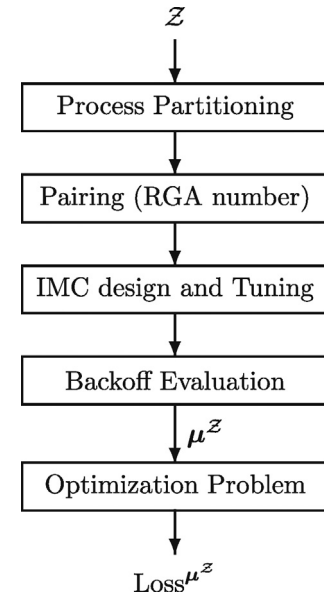


Fig. 2. Steps in the evaluation of the optimality loss associated with a given control structure \mathcal{Z} .

$$\text{dom } U := \{\mu | U(\mu) \neq \emptyset\}. \quad (32)$$

The constraint backoffs μ^z computed in step (d) should satisfy $\mu^z \in \text{dom } U$, otherwise, the optimization problem in step (e) does not have a feasible solution and the control structure \mathcal{Z} is unfeasible. Overall, the optimization problem can be formulated as follows:

$$\min_{\mathbf{u}, \mathcal{Z}} \text{Loss}^{\mu^z} = J(\mathbf{x}, \mathbf{w}, \mathbf{u}, \mathbf{d}_n) - J^*(\mathbf{0}, \mathbf{d}_n) \quad (33a)$$

$$\text{s.t. } \mathbf{f}_D(\mathbf{0}, \mathbf{x}, \mathbf{w}, \mathbf{u}, \mathbf{d}_n) = \mathbf{0}, \quad (33b)$$

$$\mathbf{f}_A(\mathbf{x}, \mathbf{w}, \mathbf{u}, \mathbf{d}_n) = \mathbf{0}, \quad (33c)$$

$$\mathbf{y}^L + \mu_y^z \leq \mathbf{y} = \mathcal{F}(\mathbf{x}, \mathbf{w}, \mathbf{u}, \mathbf{d}_n) \leq \mathbf{y}^U - \mu_y^z, \quad (33d)$$

$$\mathbf{u}^L + \mu_u^z \leq \mathbf{u} \leq \mathbf{u}^U - \mu_u^z, \quad (33e)$$

$$n_q \leq \min\{n_y, n_u\} \quad (33f)$$

$$\|\mathbf{c}_O\|_1 = \|\mathbf{c}_I\|_1 = n_q \quad (33g)$$

$$\mathbf{T}_O = \text{nre}[\text{diag}(\mathbf{c}_O)], \quad \mathbf{T}_I = \text{nce}[\text{diag}(\mathbf{c}_I)] \quad (33h)$$

$$\mathbf{G}_s^z(s) = \mathbf{T}_O \mathbf{G}(s) \mathbf{T}_I, \quad \mathbf{D}_s^z(s) = \mathbf{T}_O \mathbf{D}(s) \quad (33i)$$

$$\mathbf{G}_r^z(s) = \tilde{\mathbf{T}}_O \mathbf{G}(s) \mathbf{T}_I, \quad \mathbf{D}_r^z(s) = \tilde{\mathbf{T}}_O \mathbf{D}(s) \quad (33j)$$

$$\tilde{\mathbf{G}}_s^{z\Gamma}(s) = \tilde{\mathbf{G}}_s^z(s) \otimes \Gamma \quad (33k)$$

Diagonal input–output pairing of $\mathbf{G}_s(s)$ and $\tilde{\mathbf{G}}_s^z(s)$ by solving Problem (8) (33l)

$$\text{Re} \left[\lambda_i \left(\mathbf{G}_s \left(\tilde{\mathbf{G}}_s^{z\Gamma} \right)^{-1} \right) \right] > 0, \quad i = 1, \dots, n_q \quad (33m)$$

$$f_{ii}(s) = 1/(\tau_f^{ii}s + 1), \quad \forall i = 1, \dots, n_q \quad (33n)$$

$$\mathbf{G}_c^z(s) = (\tilde{\mathbf{G}}_s^{z\Gamma}(s))^{-1} \mathbf{F}(s) \quad (33o)$$

$$\mathbf{B}_s^z(s) = [\mathbf{I} + (\mathbf{G}_s^z(s) - \tilde{\mathbf{G}}_s^z(s)) \mathbf{G}_c^z(s)]^{-1} \mathbf{D}_s^z(s) \quad (33p)$$

$$\Psi^z(s) = (\mathbf{I} - \mathbf{F}(s)) \mathbf{B}_s^z(s) \quad (33q)$$

$$\boldsymbol{\Xi}^Z(s) = \mathbf{D}_r^Z(s) - \mathbf{G}_r^Z(s)\mathbf{G}_c^Z(s)\mathbf{B}_s^Z(s) \quad (33r)$$

$$\boldsymbol{\Upsilon}^Z(s) = -\mathbf{G}_c^Z(s)\mathbf{B}_s^Z(s) \quad (33s)$$

$$\boldsymbol{\mu}^Z = \begin{bmatrix} \boldsymbol{\mu}_{CV}^Z \\ \boldsymbol{\mu}_{UV}^Z \\ \boldsymbol{\mu}_{MV}^Z \end{bmatrix} = \begin{bmatrix} \boldsymbol{\Psi}_\infty^Z \\ \boldsymbol{\Xi}_\infty^Z \\ \boldsymbol{\Upsilon}_\infty^Z \end{bmatrix} |_{\Delta \mathbf{d}} \quad (33t)$$

Eqs. (33f)–(33t) are all used to determine the constraint backoffs that are used in the inequality constraints (33d) and (33e). The constraints (33f) and (33g) guarantee a dimensionally feasible selection of n_q and a square control problem, respectively. The equalities shown in Eqs. (33h)–(33j) define the process partitioning based on the transformation matrices \mathbf{T}_0 and \mathbf{T}_1 , which are a function of \mathbf{c}_0 and \mathbf{c}_1 , respectively. Notice that $\tilde{\mathbf{T}}_0$ is a function of the binary complement (logical not) of \mathbf{c}_0 . All the transformation matrices are computed as indicated in Eq. (7). Eq. (33k) defines the IMC controller interaction according to the binary variable v . If $v = 0$, then a decentralized control structure is selected and $\Gamma = \Gamma_d$ is a diagonal unitary matrix of size $n_q \times n_q$. On the other hand, $v = 1$ corresponds to a full IMC controller for which $\Gamma = \Gamma_f$ is a $n_q \times n_q$ matrix with all its entries equal to one.

The steady-state stability criterion in Eq. (33m) and the low-pass filter setting in Eq. (33n) allow to guarantee the feasibility of the IMC controller design given by Eq. (33o), based on the model computed in Eq. (33k). The diagonal pairing helps the tuning procedure suggested in Eq. (33n) where $f_{ii}(s) = 1/(\tau_f^{ii}s + 1)$ is the i th component in the main diagonal of the low-pass filter matrix $\mathbf{F}(s)$, with $\tau_f^{ii} = \tau_m^{ii}/v$, $v > 0$, and τ_m^{ii} is the time constant of the (i, i) model component $\tilde{\mathbf{g}}_i^\Gamma(s)$.

The closed-loop MTFs corresponding to the net load matrix, the controlled variables, the uncontrolled variables, and the manipulated variables, are given in Eqs. (33p)–(33s). Note that these matrices correspond to the gain matrices of the corresponding sets of variables with respect to disturbance variations.

The backoff estimation is given in Eq. (33t). Clearly, this estimation is an implicit function of the control structure decision variables $[\mathbf{c}_0, \mathbf{c}_1, n_q, v]$ and it depends on the disturbance range $|\Delta \mathbf{d}|$. Note that any feasible solution to Problem (33) must satisfy $\boldsymbol{\mu} \in \text{dom } U$.

3.4. Implementation aspects

It is clear that the number of potential control structures grows quickly with the process dimension. While for small-scale systems Problem (33) results relatively easy to solve, for medium or large scale processes the problem becomes extremely hard to solve. The decision variables of Problem (33) consist of integer (binary) variables that define the control structure, and continuous variables that define the steady-state operating point of the process (the input variables).

Problem (33) corresponds to a mixed-integer nonlinear program (MINLP). However, it presents two main difficulties that need to be addressed by any solution approach:

- (i) Computing the input–output pairing in (33l) requires solving an integer optimization problem that is embedded in Problem (33).
- (ii) A dynamic simulation based on a linear dynamic model is embedded in the optimization problem in order to compute the constraint backoffs. This dynamic simulation is performed in the frequency domain, and the backoffs are computed in (33t) by evaluating the infinite norms in the frequency domain.

In order to solve Problem (33) as an MINLP, these internal algorithms need to be reformulated as equations. Since Problem (8) cannot be written as equations, a reformulation of Problem (33) is necessary in order to include decisions about the input–output pairing. This can be done by augmenting Z with the pairing variables \mathbf{P}_a , and including a lower bound on the RGA number. On the other hand, the computation of the infinite norms in (33t) requires selecting an ad-hoc grid of frequencies at which the closed-loop responses of the process variables are evaluated. These frequency responses need to be separated into their real and imaginary parts, and their magnitude in the complex plane needs to be calculated in order to compute the required infinite norms.

Due to the aforementioned difficulties in solving Problem (33) as a MINLP, an alternative sequential solution approach based on Genetic Algorithms (GA) is presented in Section 4. For any control structure Z , the evaluation of the loss is seen by the optimizer as an input–output black-box relationship, which is computed following the steps shown in Fig. 2. Whenever a control structure is infeasible, it is eliminated by assigning to it a very large loss. Note that stochastic global search approaches based on GAs have already been proposed for solving MINLP control structure selection problems of similar complexity to Problem (33), applied to medium/large scale processes [10,22,23,30].

In addition, a solution approach using a MINLP formulation is reported in Appendix A that uses the OPTimization Interface (OPTI) Toolbox [24] and the BONMIN solver [25,26].

3.5. Discussion

The estimated backoff vector depends on the disturbance range ($|\Delta \mathbf{d}|$) considered, the control structure selected, and the controller tuning adopted. These three elements directly affect the regulator behavior of the overall closed-loop system, and thereby the maximum excursion of the selected CVs and MVs. Moreover, for a given control structure, an aggressive controller setting improves the regulator performance by decreasing the maximum peak values in the CVs ($\boldsymbol{\mu}_{CV}$), but the energy required for the corresponding MVs increases ($\boldsymbol{\mu}_{MV}$). This might call for a compromise from the backoff point of view. In general, the disturbance range is fixed a priori, leaving only two handles for minimizing the maximum temporal excursions ($\boldsymbol{\mu}$) of the process variables: the choice of the control structure and the controller tuning. Note that for a given feasible control structure the corresponding tuning of the controller is not free. Indeed, the selected tuning must meet some stability/robustness criteria, i.e., it cannot be obtained based only on steady-state economic criteria.

The backoff estimation approach is subject to the inherent limitations of using simplified linear models. If the disturbance magnitudes are severe, the process model can lose its validity producing wrong estimations of $\boldsymbol{\mu}$. The introduction of robustness in the evaluation of the constraint backoffs should be considered in order to prevent constraint violations. In this work, the backoffs corresponding to the control structure obtained by solving Problem (33) where recomputed by incorporating input multiplicative uncertainty, as described in Section 3.2. Note that, another way around would be to directly incorporate the uncertainty description in the model used in Problem (33).

4. Illustrative case study

4.1. Evaporator process

The well-known forced-circulation evaporator described by Newell and Lee [27] is used here to illustrate the previously presented plantwide control design based on robust backoff

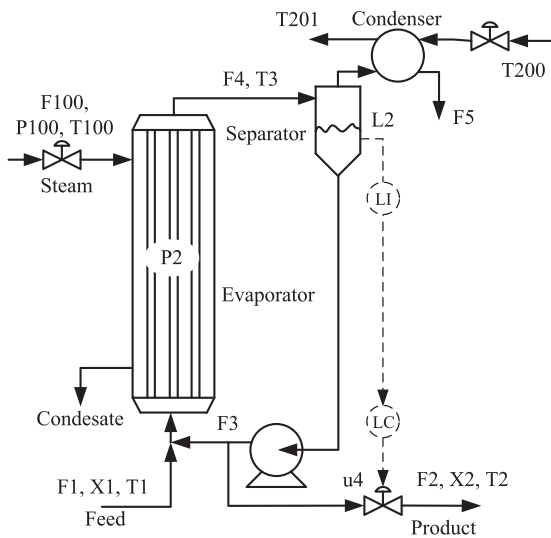


Fig. 3. Evaporator system.

evaluation. The layout of the evaporator with its corresponding stabilizing control loop is shown in Fig. 3. The evaporator is fed by a mixture of fresh liquid feed and recirculating liquor. This mixture boils inside the evaporator, which is heated by steam. The generated vapor–liquid mixture is separated in a separator. The overhead vapor is condensed by means of a heat exchanger. Most of the separated liquid becomes the recirculating liquor, and a small proportion of it is drawn off as product. This product is more concentrated than the fresh liquid feed. It is worth mentioning that the process is open-loop unstable due to the integrating behavior of the separator's level L_2 . In order to stabilize the system, a control loop is introduced that controls the level L_2 by manipulating the product flow rate F_2 . This case study has been used by several researchers for testing new developments in the areas of self-optimizing control [28,29], plant-wide control [19], and control structure selection using the backoff approach [4], among others. The same operating cost and constraints of the evaporator as suggested by Heath et al. [4] are used here for illustrating our methodology. The open-loop nonlinear dynamical model is given by:

$$\begin{aligned} \rho A \frac{dL_2}{dt} &= F_1 - F_4 - F_2 \\ M \frac{dX_2}{dt} &= F_1 X_1 - F_2 X_2 \\ C \frac{dP_2}{dt} &= F_4 - F_5 \end{aligned} \quad (34)$$

with

$$\begin{aligned} F_4 &= 0.16(F_1 + F_3)(-0.3126X_2 - 0.5616P_2 + 0.1538P_{100} + 41.57) / \lambda_{s1} - C_p F_1 (0.3126X_2 + 0.5616P_2 + 48.43 - T_1) / \lambda_{s1} \\ F_5 &= 2U A_2 C_p F_{200} (0.507P_2 + 55 - T_{200}) / (\lambda_{s2} (U A_2 + 2C_p F_{200})) \\ T_{100} &= 0.1538P_{100} + 90 \\ T_2 &= 0.5616P_2 + 0.3126X_2 + 48.43 \\ T_3 &= 0.507P_2 + 55 \\ F_{100} &= (F_1 + F_3)(T_{100} - T_2)0.16 / \lambda_{s1} \end{aligned} \quad (35)$$

The main process variables are listed in Table 1, and the process parameters are defined as $\rho A = 20 \text{ kg/m}$, $M = 20 \text{ kg}$, $C = 4 \text{ kg/KPa}$, $U A_2 = 6.84 \text{ Kw/K}$, $C_p = 0.07 \text{ Kw/kg min}$, $\lambda_{s1} = 36.6 \text{ Kw/kg min}$,

Table 1
Main process variables and nominal operating point.

	Description	Value	Unit
<i>Outputs</i>			
X_2	Product composition	35	[%]
P_2	Operating pressure	56.208	[kPa]
F_4	Vapor flow rate	8.571	[kg/min]
F_5	Condensate flow rate	8.571	[kg/min]
T_2	Product temperature	90.9	[°C]
T_3	Vapor temperature	83.5	[°C]
F_{100}	Steam flow rate	9.546	[kg/min]
<i>Inputs</i>			
P_{100}	Steam pressure	400	[kPa]
F_{200}	Cooling water flow rate	229.927	[kg/min]
F_3	Recirculation flow rate	26.043	[kg/min]
<i>Disturbances</i>			
F_1	Feed flow rate	10	[kg/min]
X_1	Feed composition	5	[%]
T_1	Feed temperature	40	[°C]
T_{200}	Cooling water inlet temperature	25	[°C]
Cost: J	Operating cost	5893.057	[\$/h]

$\lambda_{s2} = 38.5 \text{ Kw/kg min}$. The steady-state optimization problem is formulated as follows:

$$\min_{\mathbf{u}} J = 1.009(F_2 + F_3)(T_{100} - T_2) + \frac{96(F_1 + F_3)(T_{100} - T_2)}{\lambda_{s1}} + 0.6F_{200} \quad (36a)$$

$$\text{s.t. Steady-state model equations,} \quad (36b)$$

$$g_1 = 35 - X_2 + \mu_1 \leq 0, \quad (36c)$$

$$g_2 = 40 - P_2 + \mu_2 \leq 0, \quad (36d)$$

$$g_3 = P_2 - 80 + \mu_3 \leq 0, \quad (36e)$$

$$g_4 = P_{100} - 400 + \mu_4 \leq 0, \quad (36f)$$

$$g_5 = F_{200} - 400 + \mu_5 \leq 0. \quad (36g)$$

The input (decision) variables are $\mathbf{u} = [P_{100} \ F_{200} \ F_3]^T$. The evaporator operating cost, in (36a), is expressed in [\$/h], and it considers the costs associated with the use of electricity, steam, and cooling water [4]. The steady-state model in (36b) corresponds to the steady-state version of Eq. (34), together with Eq. (35). The main objective is to minimize J subject to the inequality constraints (36c)–(36g). The first three constraints involve the output variables X_2 and P_2 , thus, the associated backoff subset results $\boldsymbol{\mu}_O = [\mu_1 \ \mu_2 \ \mu_3]^T$ with $\mu_2 = \mu_3$. On the other hand, the last two constraints refer to the input variables, P_{100} and F_{200} , for which the corresponding backoff vector is $\boldsymbol{\mu}_I = [\mu_4 \ \mu_5]^T$. Both, the output and input backoff subsets can be collected in a single vector $\boldsymbol{\mu} = [(\boldsymbol{\mu}_O)^T \ (\boldsymbol{\mu}_I)^T]^T$.

As indicated in Table 1, the nominal disturbance values are $\mathbf{d}_n = [10 \text{ kg/min}, 5\%, 40^\circ\text{C}, 25^\circ\text{C}]^T$. The nominal operating point, which is shown in Table 1, is obtained by solving Problem (36a) for $\mathbf{d} = \mathbf{d}_n$ and $\boldsymbol{\mu} = \mathbf{0}$. Note that, at the nominal optimum the product composition X_2 is active at its lower bound, and the steam pressure P_{100} is active at its upper bound. That is, the output constraint g_1 and the input constraint g_4 are both active.

Using the description of the variables defined in Table 1, a linear model of the process has been identified at the nominal operating point. This model is given by the following MTFs $\mathbf{G}(s)$ and $\mathbf{D}(s)$, which correspond to the input–output and disturbance–output

mappings, respectively.

$$\mathbf{G}(s) = \begin{bmatrix} 0.1706 & 0.056 & 1.7893 \\ (5s+1) & (35s+1) & (5s+1) \\ 0.0853 & -0.0538 & 0.9212 \\ (30s+1) & (35s+1) & (25s+1) \\ 0.0063 & 0.022 & 0.0685 \\ (s+1) & (25s+1) & (s+1) \\ 0.0063 & 0.022 & 0.0685 \\ (30s+1) & (s+1) & (25s+1) \\ 0.1012 & -0.0127 & 1.0767 \\ (5s+1) & (25s+1) & (5s+1) \\ 0.0433 & -0.0273 & 0.4671 \\ (30s+1) & (35s+1) & (25s+1) \\ 0.0083 & 0.0020 & 0.0891 \\ (s+1) & (25s+1) & (s+1) \end{bmatrix},$$

$$\mathbf{D}(s) = \begin{bmatrix} -10.5786 & 4.3812 & 0.1276 & -1.2617 \\ (10s+1) & (15s+1) & (5s+1) & (40s+1) \\ 4.3472 & -1.3944 & 0.0696 & 1.2458 \\ (35s+1) & (40s+1) & (25s+1) & (35s+1) \\ 0.3232 & -0.1036 & 0.0052 & -0.0539 \\ (5s+1) & (3s+1) & (s+1) & (30s+1) \\ 0.3232 & -0.1036 & 0.0052 & -0.0539 \\ (35s+1) & (40s+1) & (25s+1) & (s+1) \\ -0.8654 & 0.5864 & 0.0790 & 0.3052 \\ (3s+1) & (3s+1) & (5s+1) & (30s+1) \\ 2.2042 & -0.7068 & 0.0353 & 0.6317 \\ (35s+1) & (40s+1) & (30s+1) & (35s+1) \\ 0.4032 & -0.0924 & -0.0124 & -0.0481 \\ (3s+1) & (3s+1) & (5s+1) & (30s+1) \end{bmatrix} \quad (37)$$

The linear model in Eq. (37) was obtained via step-test identification experiments for the stabilized non-linear model of the evaporator process around the nominal working point. For simplicity, first-order transfer functions without dead time information were selected for each component.

As indicated in Table 1, this linear model presents $n_y = 7$ output variables, $n_u = 3$ available MVs, and $n_d = 4$ disturbances. Considering the overall problem stated in Section 3.3, in this case, there are 273 potential control structures (CSs):

- 21 (1×1) SISO control policies,
- 252 (2×2) MIMO control structures: 126 full + 126 decentralized.

Note that in [4] the recirculation flow rate F_3 is considered as a disturbance, and only X_2 and P_2 are considered as potential controlled variables. In contrast, in this work F_3 is incorporated as a potential manipulated variable, and the number of potential controlled variables is equal to seven. Therefore, the number of potential control structures considered in this work is much larger than those considered in Heath et al. [4].

A particular control structure is defined by means of the parameterization vector $\mathcal{Z} = [\mathbf{c}_0, \mathbf{c}_I, n_q, v]$, with $n_q \in \{1, 2\}$. Any given control structure \mathcal{Z} has an associated constraint backoff vector $\mu^{\mathcal{Z}}$. The evaluation of $\mu^{\mathcal{Z}}$ requires using a predefined disturbance range $\Delta\mathbf{d}$. Here, the same disturbance range as suggested by Heath et al. [4] is used:

$$\begin{aligned} |\Delta\mathbf{d}|^T &= [|\Delta d_1| \, |\Delta d_2| \, |\Delta d_3| \, |\Delta d_4|]^T \\ &= [0.05\text{kg } 0.25\% \, 2.00^\circ\text{C } 1.25^\circ\text{C}]^T. \end{aligned} \quad (38)$$

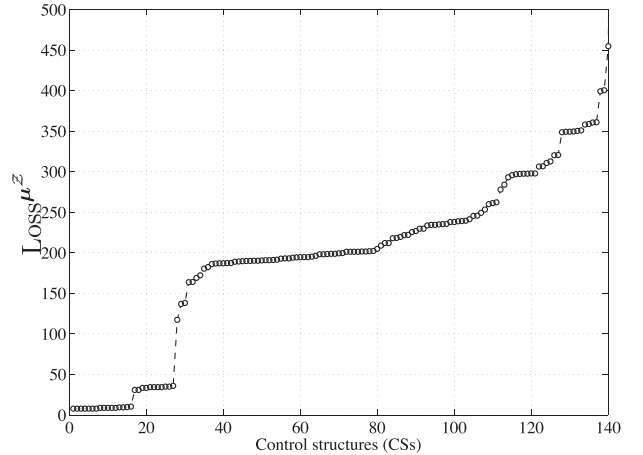


Fig. 4. Exhaustive evaluation of control structures for the evaporator process.

Exhaustive search. Due to the small dimensions of evaporator system under study, it is not prohibitive in this case to evaluate exhaustively all the possible SISO and 2×2 MIMO control structures. The exhaustive evaluation of the 273 potential control structures results in 140 feasible control structures, 48 unfeasible policies which violate the constraint in Eq. (33m), and 85 unfeasible structures that do not satisfy $\mu^{\mathcal{Z}} \in \text{dom } U$. Fig. 4 shows the loss profile for all the 140 feasible solutions found. The solutions are sorted from the best (left) to the worst (right).

Solution strategy based on genetic algorithms. A generic approach to the solution of Problem (33) can be implemented by defining the control structure $\mathcal{Z} = [\mathbf{c}_0, \mathbf{c}_I, n_q, v]$ as the integer decision variables for the genetic algorithm (GA) optimiser, and by using the sequential procedure described in Fig. 5 in order to evaluate the associated loss. This loss is handled by the GA procedure as the fitness function (input–output blackbox relationship) for evolving towards the new generation. The procedure is repeated until a stopping criteria is reached. Whenever a control structure is infeasible, it is eliminated by assigning to it a very large loss Loss^H . In this case, the GA function from the global optimization toolbox of Matlab was implemented with five generations as stopping criterion and 12 integer decision variables. The overall optimization time was approximately 7 min (Intel Core i5, 3.1 GHz, 4GB RAM, 64 bits), and the best solution found agrees with the optimal solution found in the exhaustive search.

Selected control structures. The most representative control structures are selected from Fig. 4. The five selected policies are indicated in Table 2, where “CS*i*” stands for the *i*th solution in the profile of Fig. 4. Note that the vector \mathbf{P}_a includes the column permutations required for the steady-state process matrix \mathbf{G} to give diagonal input–output pairing. The selected policies have the following description:

- CS1: the best (2×2) “decentralized” control structure, wherein X_2 and T_3 are the CVs and F_3 and F_{200} are the corresponding MVs.
- CS3: the best (2×2) “full” control structure, wherein X_2 and T_2 are the CVs and F_3 and F_{200} are the corresponding MVs.
- CS4: the best (1×1) control structure, wherein X_2 and F_3 are the CV and MV, respectively.
- CS15: the second best (1×1) control structure, wherein X_2 and P_{100} are the CV and MV, respectively.
- CS23: the third best (1×1) control structure, wherein X_2 and F_{200} are the CV and MV, respectively.

Table 3 presents the computed values of the estimated backoffs and the associated loss evaluation for each of the CSs defined in

Table 2

Selected CSs from Fig. 4.

CSs	\mathbf{C}_O						\mathbf{C}_I			n_q	v	\mathbf{P}_d		
	X_2	P_2	F_4	F_5	T_2	T_3	F_{100}	P_{100}	F_{200}	F_3				
CS1	1	0	0	0	0	1	0	0	1	1	2	0	2	1
CS3	1	0	0	0	1	0	0	0	1	1	2	1	2	1
CS4	1	0	0	0	0	0	0	0	0	1	1	0	–	–
CS15	1	0	0	0	0	0	0	1	0	0	1	0	–	–
CS23	1	0	0	0	0	0	0	0	1	0	1	0	–	–

Table 3

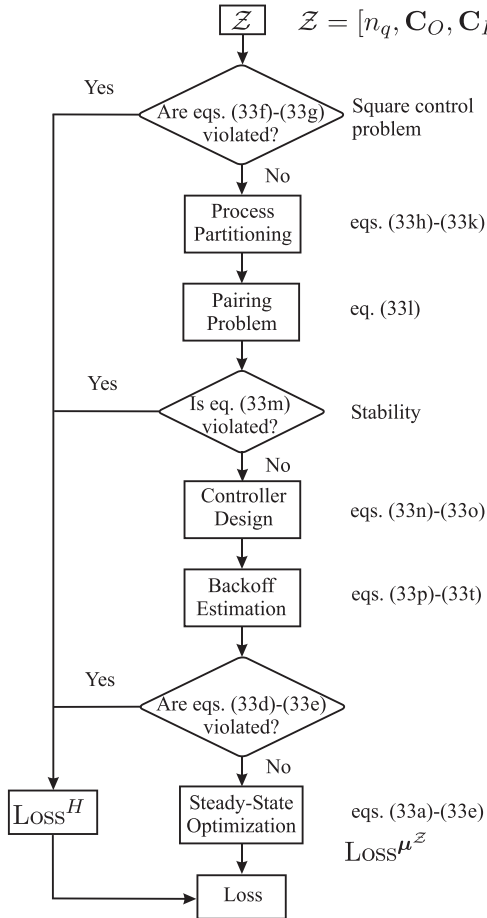
Back-off estimation and loss evaluation.

	Open loop	Control structures				
		CS1	CS3	CS4	CS15	CS23
$J^*(\mu^Z, d_n)$	5995.431	5900.6938	5900.7675	5900.7678	5902.7507	5927.3348
Loss^{μ^Z}	102.374	7.6361	7.7098	7.7101	9.6930	34.2771
μ_1	3.456	0.2389	0.2413	0.2413	0.2413	1.0953
$\mu_2 = \mu_3$	2.262	5.7750	4.7239	4.0420	3.9907	7.0290
μ_4	0.000	0.0000	0.0000	0.0000	20.2612	0.0000
μ_5	0.000	49.7995	19.7237	0.0000	0.0000	88.2991

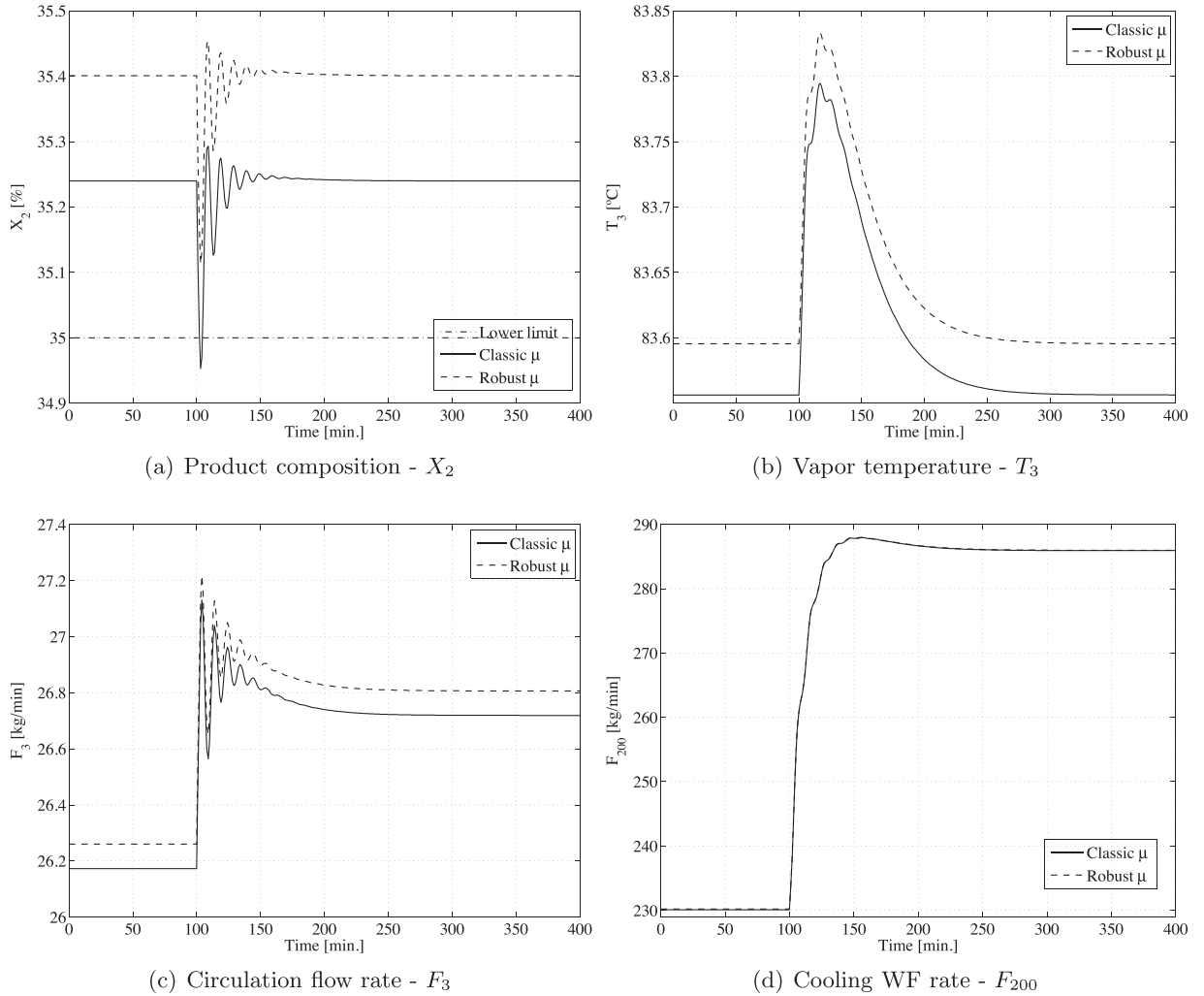
Table 2. In addition, for comparative purposes, the backoff values and the associated loss are also displayed for the open loop case. Notice that, if a constrained input variable is not used for control purposes (i.e., it is not selected as a MV), then it is fixed at its nominal value and its corresponding backoff value in μ_l^Z is fixed to zero. From Table 3 it can be seen that CS1 and CS3 have very similar loss values.

Some authors do not consider F_3 as a MV but rather as a disturbance [4]. The solution CS15 was selected because it represents the best SISO control structure when the variable F_3 is not used as a MV. Notice that if F_3 is not a MV, then the evaporator system comprises two MVs and two active constraints. In optimizing control, the typical or common sense selection would consist in controlling both active constraints [31,32]. In our case, this implies fixing the input P_{100} at its active upper bound value, and controlling the product composition X_2 at its active upper bound value by manipulating the remaining input F_{200} . This selection corresponds to the solution CS23. From Table 3 it can be seen that the optimizing control structure CS23 requires larger constraint backoffs than the solution CS15, and thus it has a higher nominal loss of 34.283. Instead of fixing the constrained input P_{100} at its active boundary value of 400 kPa, the control structure CS15 selects P_{100} as a MV by setting a suitable backoff value. Selecting P_{100} as a MV permits to decrease the constraint backoff required for the active output constrained variable X_2 . Since the Lagrange multiplier associated with X_2 ($\nu_1 = 32.15$) is much larger than the Lagrange multiplier associated with P_{100} ($\nu_4 = 0.0923$), it turns out that decreasing the constraint backoff on X_2 is much more important in terms of optimality than decreasing (zeroing) the constraint backoff on P_{100} .

In Section 3.2 we discussed the need to introduce robustness in the estimation of the constraint backoffs, and we proposed analyzing the problem under multiplicative input uncertainty. A robust estimation of the constraint backoffs is performed next for CS1 and CS15, by introducing multiplicative input uncertainty. The computed conservative values of the constraint backoffs and the associated loss are given in Table 4. The parameters of the weighting functions used for each input channel u_j are shown in Table 5, according to the discussion in

**Fig. 5.** Sequential procedure for the loss evaluation (fitness function) used by the genetic algorithm.**Table 4**
Robust back-off estimation and loss evaluation – CS1/CS15.

	Control structures	
	CS1	CS15
$J^*(\mu^Z, d_n)$	5905.7456	5907.6955
Loss^{μ^Z}	12.6879	14.6378
μ_1	0.3986	0.3882
$\mu_2 = \mu_3$	6.4696	4.2263
μ_4	0.0000	23.0234
μ_5	58.3362	0.0000

**Fig. 6.** CS1 – decentralized (2×2).

Sections 2.3.1 and 3.2, i.e. $1/\tau^j > 1/\tau_f^{ij} = v^{ij}/\tau_{ij}$. Notice that τ_{ij} is the time constant of the associate model component $\tilde{g}_{ij}(s)$. It is clear that the input uncertainties affect the backoff estimation depending on the CS selected for the process. Furthermore, this new estimation of μ gives a new optimality loss value for each control policy. A comparison of Tables 3 and 4 shows that by

introducing multiplicative input uncertainty the control structures CS1 and CS15 increase their optimality loss in 66.15 % and 51.01 %, respectively.

The dynamic behavior of the process when the control structures CS1 and CS15 are implemented is shown in Figs. 6 and 7, respectively. All the simulations are conducted using the nonlinear

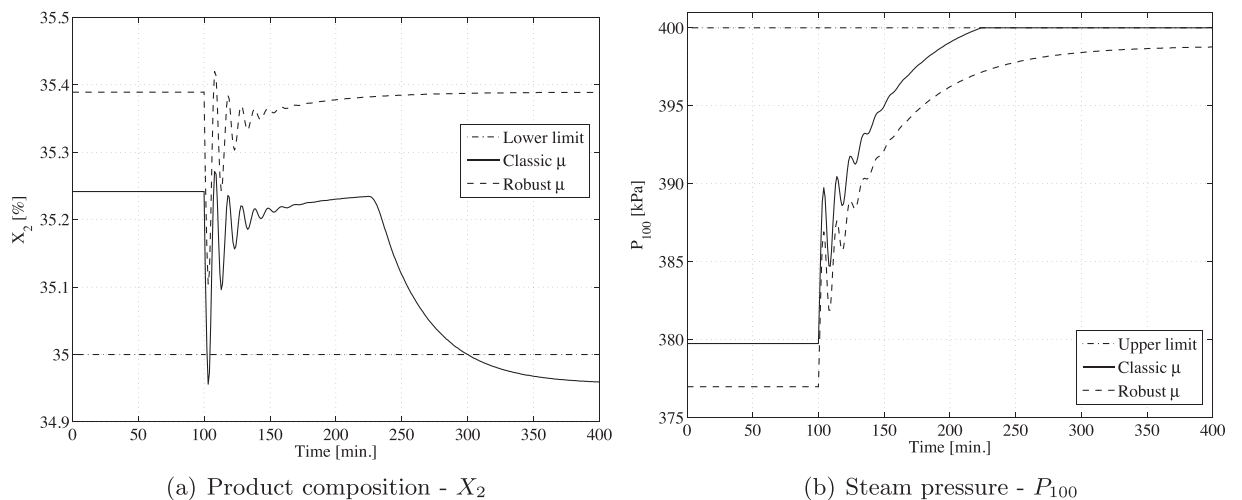
**Fig. 7.** CS15 – SISO (1×1).

Table 5

Parameters of the weighting function for each input channel.

Channel	r_0^j [%]	r_∞^j [%]	$1/\tau^j$ [rad/min]	v^{ij}	ν^j
u_j	10	200	$v^{ij}/\tau_{ij} + \nu^j$	4	0.4

process model, and for each control structure the scenarios with and without robust backoff estimation are shown. In all the simulations, the disturbance $\Delta d = [0.05, -0.25, -2, 1.25]^T$ takes place at time $t = 100$ min. This disturbance is within the disturbance range used to evaluate the constraint backoffs (see Eq. (38)). Without a robust backoff estimation, the control structure CS1 presents some problems to maintain the product composition X_2 within the feasible operation zone during the transient. This undesired behavior clearly disappears when the robust evaluation of μ is used. The benefits of the robust estimation of the constraint backoffs can also be clearly seen for the control structure CS15 in Fig. 7. Without introducing robustness, the MV P_{100} saturates at its upper limit, which produces the loss of control on the product composition X_2 . In contrast, the robust estimation guarantees the process operation within the feasible region.

5. Conclusions

In this work, the constraint backoff approach was considered for the selection of process control structures based on economics. A procedure was presented for implementing the backoff approach based on IMC control theory for parametrizing the controller and computing the required dynamic constraint backoffs. IMC provides a suitable representation from the controller interaction as well as the stability and robustness points of views. In fact, the IMC framework enables to represent decentralized, sparse, and full controller interaction. For simplicity, only decentralized and full control policies were considered here.

The strategy described in this paper is a model-based approach. Therefore, its reliability depends on the accuracy of the process model, and the correct choice of the disturbance vector. The optimization problem to be solved consists in a non-convex MINLP. In this paper, we have tackled this problem using a sequential solution approach based on Genetic Algorithms. In the Appendix, a solution approach using the OPTI Toolbox is also reported. The investigation of a more rigorous solution approach will require future work.

The process evaporator case study was used to illustrate the approach and to compare different solution strategies. The dynamic simulations conducted on the system show that in the presence of disturbances the backoffs computed based on a linearized dynamic model can result in constraint violations during the transient, or in the saturation of the controller at steady state. In order to prevent this, robustness in the evaluation of the backoffs was introduced by considering input multiplicative uncertainty.

Finally, the results show that the economic based criterion of minimizing the nominal loss (17) does not necessarily lead to the standard optimizing control strategy of controlling all the active constraints. In particular, rather than fixing an active constrained input to its optimal limit value, it might be more profitable in some cases to use it as a manipulated variable in order to reduce the variability of other constrained variables.

Acknowledgements

The authors thank the financial support of CIFASIS-CONICET, ANPCYT (PICT 2012-0133), UNR, and UTN-FRRo from Argentina.

Table A.6

OPTI toolbox implementation – problem properties.

Decision variables	Bounds	Integer variables	Nonlinear inequality	Nonlinear equality
25	50	20	8	8

Table A.7

OPTI toolbox implementation – solution given by BONMIN.

C_0						C_I			P_a	Loss $^{\mu^Z}$		
X_2	P_2	F_4	F_5	T_2	T_3	F_{100}	P_{100}	F_{200}	F_3			
1	0	0	0	1	0	0	0	1	1	2	1	7.8057

Appendix A. MINLP implementation example – OPTI toolbox

In this section, a simplified version of Problem (33) is solved for the evaporator case study based on deterministic optimization tools. The environment used in this case is the OPTimization Interface (OPTI) Toolbox, which permits to construct and solve linear, nonlinear, continuous and discrete optimization problems by linking the benefits from Matlab programming with the most of popular open source and academic optimization solvers [24]. In this case, the BONMIN (Basic Open Source Nonlinear Mixed Integer Programming) [25,26] tool was used, which presents several algorithmic choices to address MINLP problems such as: B-BB, a NLP-based branch-and-bound algorithm; B-OA, an outer-approximation decomposition algorithm; B-iFP, an iterated feasibility pump algorithm; B-QG a branch-and-cut algorithm; and B-Hyb, a hybrid outer-approximation based branch-and-cut algorithm. It is worth mentioning that the different methods that BONMIN implements are exact algorithms when the cost as well as the constraint functions are convex, but are only heuristics when this is not the case (i.e. BONMIN is not a global optimizer). This is the major drawback of the solver and since Problem (33) is nonlinear, it is possible that the solution found will be suboptimal.

A simplified version of Problem (33) applied to the evaporator process is considered. In this case, only (2×2) control structures are selected, whereby $n_q = 2$ and $v = 0$ are fixed. In this context, Problem (33) is solved simultaneously, instead of using the sequential procedure shown in Fig. 5. The general properties of the optimization problem are presented in Table A.6. The solvers named as B-BB, B-OA, B-QG, B-Hyb, and B-iFP were evaluated (Intel Core i5, 3.1 GHz, 4GB RAM, 64 bits), giving the optimization times (minutes) 7.1819, 3.6438, 3.4157, 3.2560, and 18.5421, respectively. All the solvers suggest the same optimal solution, which is shown in Table A.7 with Loss $^{\mu^Z} = 7.8057$. This corresponds to a suboptimal solution since the solution given by the exhaustive search, as well as the global optimization via GA, gives Loss $^{\mu^Z} = 7.6361$, as shown in Table 3.

References

- [1] S. Skogestad, I. Postlethwaite, *Multivariable Feedback Control. Analysis and Design*, John Wiley & Sons, 2005.
- [2] G.P. Rangaiah, V. Karriwala, *Plantwide Control. Recent Developments and Applications*, John Wiley and Sons Ltd, 2012.
- [3] J. Downs, S. Skogestad, An industrial and academic perspective on plantwide control, *Annu. Rev. Control* 35 (2011) 99–110.
- [4] J. Heath, I. Kookos, J. Perkins, Process control structure selection based on economics, *AIChE J.* 46 (10) (2000) 1998–2016.
- [5] N. Chawankul, H. Budman, P. Douglas, The integration of design and control: IMC control and robustness, *Comput. Chem. Eng.* 29 (2005) 261–271.
- [6] C. Swartz, The use of controller parameterization in the integration of design and control, in: P. Seferlis, M.C. Georgiadis (Eds.), *The Integration of Process Design and Control*, Elsevier B.V., 2004.
- [7] C. Loeblein, J.D. Perkins, Structural design for on-line process optimization: I. Dynamic economics of MPC, *AIChE J.* 45 (5) (1999) 1018–1029.

- [8] S. Bahakim, L. Ricardez-Sandoval, Simultaneous design and MPC-based control for dynamic systems under uncertainty: a stochastic approach, *Comput. Chem. Eng.* 63 (2014) 66–81.
- [9] M. Morari, E. Zafiriou, *Robust Process Control*, Prentice Hall, New York, 1989.
- [10] D. Zumoffen, Oversizing analysis in plant-wide control design for industrial processes, *Comput. Chem. Eng.* 59 (2013) 145–155.
- [11] M.J. Mohideen, J.D. Perkins, E.N. Pistikopoulos, Optimal design of dynamic systems under uncertainty, *AIChE J.* 42 (8) (1996) 2251–2272.
- [12] V. Sakizlis, J.D. Perkins, E.N. Pistikopoulos, Recent advances in optimization-based simultaneous process and control design, *Comput. Chem. Eng.* 28 (2004) 2069–2086.
- [13] L.A. Ricardez-Sandoval, H.M. Budman, P.L. Douglas, Integration of design and control for chemical processes: a review of the literature and some recent results, *Annu. Rev. Control* 33 (2009) 158–171.
- [14] L.T. Narraway, J.D. Perkins, Selection of process control structure based on linear dynamic economics, *Ind. Eng. Chem. Res.* 32 (1993) 2681–2692.
- [15] L.T. Narraway, J.D. Perkins, G.W. Barton, Interaction between process design and process control: economic analysis of process dynamics, *J. Process Control* 1 (1991) 243–250.
- [16] A. Psaltis, I.K. Kookos, C. Kravaris, Plant-wide control structure selection methodology based on economics, *Comput. Chem. Eng.* 52 (2013) 240–248.
- [17] C. Garcia, M. Morari, Internal model control. 2. Design procedure for multivariable systems, *Ind. Eng. Chem. Process Des. Dev.* 24 (1985) 472–484.
- [18] C. Garcia, M. Morari, Internal model control. 1. A unifying review and some new results, *Ind. Eng. Chem. Process Des. Dev.* 21 (1982) 308–323.
- [19] D. Zumoffen, M. Basualdo, Improvements on multiloop control design via net load evaluation, *Comput. Chem. Eng.* 50 (2013) 54–70.
- [20] I.K. Kookos, J.D. Perkins, An algorithmic method for the selection of multivariable process control structures, *J. Process Control* 12 (2002) 85–99.
- [21] B. Chachuat, A. Marchetti, D. Bonvin, Process optimization via constraints adaptation, *J. Process Control* 18 (2008) 244–257.
- [22] M. Sharifzadeh, N. Thornhill, Optimal selection of control structure using a steady-state inversely controlled process model, *Comput. Chem. Eng.* 39 (2012) 126–138.
- [23] P. Luppi, D. Zumoffen, M. Basualdo, Decentralized plantwide control strategy for large-scale processes. Case study: pulp mill benchmark problem, *Comput. Chem. Eng.* 52 (2013) 272–285.
- [24] J. Currie, D. Wilson, OPTI: lowering the barrier between open source optimizers and the industrial MATLAB user, in: *Foundations of Computer-Aided Process Operations (FOCAPO)*, Savannah, GA, USA, 2012.
- [25] P. Bonami, J. Lee, *BONMIN Users' Manual*, 2013 www.coin-or.org/Bonmin.
- [26] P. Bonami, L.T. Biegler, A.R. Conn, G. Cornuéjols, I.E. Grossmann, C.D. Laird, J. Lee, A. Lodi, F. Margot, A. Wächter, An algorithmic framework for convex mixed integer nonlinear programs, *Discrete Optim.* 5 (2008) 186–204.
- [27] R.B. Newell, P.L. Lee, *Applied Process Control: A Case Study*, Prentice Hall, Englewood Cliffs, NJ, 1989.
- [28] V. Kariwala, Y. Cao, S. Janardhanan, Local self-optimizing control with average loss minimization, *Ind. Eng. Chem. Res.* 47 (2008) 1150–1158.
- [29] A.G. Marchetti, D. Zumoffen, Self-optimizing control structures with minimum number of process-dependent controlled variables, *Ind. Eng. Chem. Res.* 53 (24) (2014) 10177–10193.
- [30] D. Zumoffen, Plant-wide control design based on steady-state combined indexes, *ISA Trans.* 60 (2016) 191–205.
- [31] A. Maarleveld, J.E. Rijnsdorp, Constraint control on distillation columns, *Automatica* 6 (1970) 51–58.
- [32] C.E. Garcia, M. Morari, Optimal operation of integrated processing systems. Part II: Closed-loop on-line optimizing control, *AIChE J.* 30 (2) (1984) 226–234.